Safe Tracking Control of Discrete-Time Nonlinear Systems Using Backward Reachable Sets

Mohamed Serry, Liren Yang, Necmiye Ozay, and Jun Liu

Abstract— **Tracking controllers are often integrated into control systems to ensure robustness against uncertainties and disturbances during trajectory following maneuvers, where the design methods in the literature lack formal guarantees, can be applied only to limited classes of systems, and/or suffer from conservatism. In this paper, we propose a new tracking control approach for discrete-time nonlinear uncertain systems using set-based computations. In particular, we compute zonotopic backward reachable sets along prescribed nominal trajectories, and utilize such sets to synthesize tracking controllers that ensure safety and reachability in the presence of input/state constraints and disturbances. We illustrate our approach through two numerical examples (Dubin's car and planar quadrotor).**

I. Introduction

Control design for safety-critical systems with reachability requirements (e.g., path planning for unmanned ground and aerial vehicles) must ensure desired specifications satisfaction, even in the presence of model nonlinearity, uncertainties, and disturbances. This is critical for system safety, yet difficult to accomplish in general. To provide some level of robustness, it is a common practice to embed tracking controllers into control systems to keep systems' states close to prescribed nominal trajectories [1], [2]. However, state/input constraints may not be fulfilled after embedding such controllers. Satisfying input/sate constraints while trajectory following may be achieved by incorporating control barrier functions to correct nominal inputs [3], though computing such functions for general nonlinear systems remains a challenging task. State-of-the-art formal methods construct tracking controllers in advance and nominal trajectories are then synthesized accordingly, where the behavior of the control system with the embedded tracking controller is taken into consideration during the trajectory synthesis. For example, in the frameworks of control contraction metrics and model predictive control [4], [5], [6], time-independent robust invariant sets with associated tracking controllers are designed, and in the subsequent trajectory planning, the safe, target, and input sets are deflated, while the unsafe sets are inflated using conservative bounds of the tracking control effort and the invariant set. Conservatism of such bounds may result in unsuccessful or low-quality trajectory generation. To mitigate the conservatism and improve the quality of the obtained trajectories, time-varying robust invariant sets are utilized [7], [8], where the designed invariant sets typically have fixed templates (e.g., ellipsoids) with time-varying scaling factors. It is worth noting that computations of such robust invariant sets are typically costly. However, these computations are done offline. In addition, the use of fixed templates for invariant sets still possesses some conservatism even in the case of time-varying invariant sets, and that cannot be avoided especially when invariant-set computations and trajectory planning are to be separated. In a recent approach, linear feedback controllers are designed and time-dependent ellipsoidal bounds of reachable sets, which are independent of the nominal trajectory, are estimated and utilized in a novel trajectory planning approach with high computational efficiency [9]. However, this recent approach is restricted to linear systems.

In this paper, we explore a new framework for tracking control that combines the practical and formal approaches, where we design tracking controllers for nonlinear systems with specified nominal trajectories, ensuring safety and input/state constraints. In fact, our method complements existing control synthesis approaches as it can be applied to arbitrary nominal trajectories, regardless of how they are generated, adding another layer of safety and robustness to existing state-of-the-art methods. In particular, we utilize and adapt the recent developments in set-based computations in order to compute zonotopic backward reachable sets along prescribed nominal trajectories of discrete-time nonlinear uncertain systems. The computed backward reachable sets can then be utilized to synthesize tracking controllers whose values are estimated online via linear feasibility problems.

Our approach can be summarized as follows: 1) We start with a prescribed nominal trajectory of a given discrete-time nonlinear system and we compute safe state and input tubes centered at the nominal states and inputs, respectively. These tubes serve two roles: first, they are utilized in estimating linearization errors (see the following point); second, the tubes serve as domains through which backward computations are conducted, while satisfying input/state constraints. 2) We linearize the dynamics of the nonlinear system along the nominal trajectory while constructing conservative estimates of the linearization error over the computed state/input tubes. 3) We proceed with under-approximate zonotopic backward reachable set computations for the conservatively linearized dynamics through the state and input tubes, starting from

M. Serry and J. Liu are with the Department of Applied Mathematics, University of Waterloo, Waterloo, Ontario, Canada. (email: {mserry, j.liu}@uwaterloo.ca).

L. Yang is with the School of Artificial Intelligence and Automation, Huazhong University of Science and Technology, Wuhan 430074, China. (email: lirenyang@hust.edu.cn).

N. Ozay is with the Department of Electrical Engineering and Computer Science, University of Michigan, Ann Arbor, MI 48105, USA (e-mail: necmiye@umich.edu).

This work was funded in part by NSERC DG, CRC, and Ontario ERA programs. Ozay is funded by NSF grants CNS-1931982 and CCF-1918123. Yang is funded by NSFC, grant No: 62320106005.

the final point of the nominal trajectory and ending at the initial point. 4) If backward computations are completed successfully, the resulting sets can be easily used to synthesize a tracking controller through solving linear feasibility problems.

The organization of this paper is as follows: the necessary preliminaries and notations are introduced in Section II, the nonlinear system under study and the associated tracking problem, with the accompanying assumptions, are presented in Section III, the proposed method is discussed thoroughly in Section IV, the method performance is illustrated through two numerical examples in Section V, and the study is concluded in Section VI.

II. Preliminaries and Notations

Let $\mathbb{R}$, $\mathbb{R}_+$, $\mathbb{Z}$, and $\mathbb{Z}_+$ denote the sets of real numbers, non-negative real numbers, integers, and non-negative integers, respectively, and $\mathbb{N} = \mathbb{Z}_+ \setminus \{0\}$. Let $[a, b]$, $]a, b[$, $[a, b[$, and $]a, b]$ denote closed, open and half-open intervals, respectively, with end points a and b, and $[a; b]$, $]a; b[$, $[a; b[$, and $]a; b]$ stand for their discrete counterparts, e.g., $[a; b] = [a, b] \cap \mathbb{Z}$, and $[1; 4[= \{1, 2, 3\}$. In $\mathbb{R}^n$, the relations $<$, $\leq$, $\geq$, and $>$ are defined component-wise, e.g., $a < b$, where $a, b \in \mathbb{R}^n$, iff $a_i < b_i$ for all $i \in [1; n]$. For $a, b \in (\mathbb{R} \cup \{-\infty, \infty\})^n$, $a \leq b$, the closed hyper-interval (or hyper-rectangle) $[\![a, b]\!]$ denotes the set $\{x \in \mathbb{R}^n \mid a \leq x \leq b\}$, where, assuming a and b are finite, $\mathrm{center}([\![a, b]\!]) := (a + b)/2$ and $\mathrm{radius}([\![a, b]\!]) := (b - a)/2$. Given $f : X \to Y$ and $C \subseteq X$, $f(C) := \{f(c) \mid c \in C\}$. The n-dimensional vectors with entries of zero and one are denoted by 0_n and 1_n, respectively. For $x \in \mathbb{R}^n$, we define $|x| = (|x_1|, \ldots, |x_n|)$, where an analogous notation is also used for matrices. Let $d = (d_1, \cdots, d_n)^\top \in \mathbb{R}^n$, then the diagonal matrix with diagonal entries $d_1, \cdots, d_n$, is denoted by $\mathrm{diag}(d)$. Given $A \in \mathbb{R}^{n \times m}$, $\mathrm{rank}(A)$ and $A^\dagger \in \mathbb{R}^{m \times n}$ denote the rank and the Moore–Penrose inverse of A, respectively. The space of n-dimensional real vectors is equipped with the maximal norm $\|\cdot\|_\infty$ ($\|x\|_\infty = \max_{i \in [1;n]} |x_i|, \ x \in \mathbb{R}^n$), and $\mathbb{B}_n$ denotes the n-dimensional closed unit ball w.r.t. $\|\cdot\|_\infty$ (i.e., $\mathbb{B}_n = [\![-1_n, 1_n]\!]$). Given $M \subseteq \mathbb{R}^n$, $\mathrm{int}(M) := \{m \in M \mid m + r\mathbb{B}_n \subseteq M \text{ for some } r > 0\}$. For $n \times m$ matrices, $\|\cdot\|_\infty$ corresponds to the matrix norm induced by the maximal norm ($\|A\|_\infty = \max_{i \in [1;n]} \sum_{j=1}^m |A_{i,j}|, \ A \in \mathbb{R}^{n \times m}$). Given $M, N \subseteq X$, $M \setminus N$ (set difference of M and N) denotes the set $\{x \in M \mid x \notin N\}$, $M + N$ (Minkowski sum of M and N) denotes the set $\{y + z \mid y \in M, z \in N\}$, and $M - N$ (Minkowski or Pontryagin difference of M and N) denotes the set $\{z \in X \mid z + N \subseteq M\}$. An important result that follows directly from the definitions of Minkowski sum and difference is the following.

Lemma 1: Let $X, Y, Z \subseteq \mathbb{R}^n$ and $A \in \mathbb{R}^{n \times n}$ be invertible. Define $S = A^{-1}((X - Y) + (-Z))$, then for all $s \in S$, there exists $z \in Z$ (that depends on s) such that $As + z + Y \subseteq X$.

Given $c \in \mathbb{R}^n$ (center), and $G \in \mathbb{R}^{n \times m}$ (generators matrix), the zonotope associated with c and G is the set $c + G\mathbb{B}_m$ (see, e.g., [10]). Note that zonotopes are closed under linear transformation and Minkowski sum as, given arbitrary zonotopes $c_1 + G_1\mathbb{B}_p, \ c_2 + G_2\mathbb{B}_q \subseteq \mathbb{R}^n$ and $A \in \mathbb{R}^{m \times n}$, $A(c_1 + G_1\mathbb{B}_p) = Ac_1 + (AG_1)\mathbb{B}_p$, and $(c_1 + G_1\mathbb{B}_p) + (c_2 + G_2\mathbb{B}_q) = (c_1 + c_2) + [G_1, G_2]\mathbb{B}_{p+q}$.

III. System Description, Assumptions, and Problem Formulation

Consider the discrete-time nonlinear system

$$x_{k+1} \in f(x_k, u_k) + \mathcal{W}, \ k \in \mathbb{Z}_+, \tag{1}$$

where $x_k \in \mathbb{R}^n$ is the state, $u_k \in \mathbb{R}^m$ is the input, $\mathcal{W} \subseteq \mathbb{R}^n$ is a disturbance set, and $f : \mathbb{R}^n \times \mathbb{R}^m \to \mathbb{R}^n$ is the function governing the unperturbed dynamics of system (1). We assume the following.

Assumption 1: The function f is twice continuously differentiable, and the matrix $D_x f(z, u) \in \mathbb{R}^{n \times n}$ is invertible for all $(z, u) \in \mathbb{R}^n \times \mathbb{R}^m$, where $D_x f$ denotes the partial derivative of f with respect to x. Note that the invertibility assumption holds if f corresponds to the flow of a continuous-time system.

Assumption 2: The disturbance set is known and given by $\mathcal{W} = [\![-\overline{w}, \overline{w}]\!]$, $\overline{w} \in \mathbb{R}^n_+$, $u_k \in \mathcal{U}$, $k \in \mathbb{Z}_+$, where $\mathcal{U}$ is known and given by $\mathcal{U} = [\![\underline{u}, \overline{u}]\!]$, and the initial value x_0 belongs to a known set $\mathcal{X}_\mathrm{i}$ given by $\mathcal{X}_\mathrm{i} = [\![\underline{x}_\mathrm{i}, \overline{x}_\mathrm{i}]\!]$.

Let $\mathcal{X}_\mathrm{o} = [\![\underline{x}_\mathrm{o}, \overline{x}_\mathrm{o}]\!] \subseteq \mathbb{R}^n$ be a hyper-rectangular operating domain and $\mathcal{X}_\mathrm{u} = \bigcup_{i=1}^{N_\mathrm{u}} [\![\underline{x}_\mathrm{u}^{(i)}, \overline{x}_\mathrm{u}^{(i)}]\!] \subseteq \mathbb{R}^n$ be an unsafe set defined as a union of N_u hyper-rectangles. It is required that the states of the system are always inside the operating domain, while avoiding the unsafe set. Let $\mathcal{X}_\mathrm{t} = [\![\underline{x}_\mathrm{t}, \overline{x}_\mathrm{t}]\!] \subseteq \mathbb{R}^n$ be a hyper-rectangular target set that we aim to drive the system's state into from the initial set $\mathcal{X}_\mathrm{i}$. We additionally assume:

Assumption 3: $\mathcal{X}_\mathrm{i} \subseteq \mathcal{X}_\mathrm{o} \setminus \mathcal{X}_\mathrm{u}$ and $\mathcal{X}_\mathrm{t} \subseteq \mathcal{X}_\mathrm{o} \setminus \mathcal{X}_\mathrm{u}$.

Let $N \in \mathbb{N}$ and $[0; N]$ be a finite-time horizon on which the reach-avoid specifications above are satisfied for the unperturbed dynamics of system (1). Specifically, let $\{\tilde{x}_k\}_{k=0}^N$ and $\{\tilde{u}_k\}_{k=0}^{N-1}$ be given nominal state and input sequences satisfying:

$$\begin{aligned} &\tilde{x}_{k+1} = f(\tilde{x}_k, \tilde{u}_k), \ k \in [0; N-1], \\ &\tilde{u}_k \in \mathcal{U}, \ k \in [0; N-1], \\ &\tilde{x}_k \in \mathrm{int}(\mathcal{X}_\mathrm{o}) \setminus \mathcal{X}_\mathrm{u}, \ k \in [0; N], \\ &\tilde{x}_0 \in \mathcal{X}_\mathrm{i}, \ \tilde{x}_N \in \mathrm{int}(\mathcal{X}_\mathrm{t}). \end{aligned} \tag{2}$$

Problem 1: Using the nominal sequences $\{\tilde{x}_k\}_{k=0}^N$ and $\{\tilde{u}_k\}_{k=0}^{N-1}$, find a control law $\mu : \mathbb{R}^n \times [0; N-1] \to \mathcal{U}$ and a set intersecting with $\mathcal{X}_\mathrm{i}$, denoted by Λ_0, such that for any initial value $z_0 \in \Lambda_0$ and any disturbance sequence $\{w_k\}_0^{N-1}$ with, $w_k \in \mathcal{W}$, $k \in [0; N-1]$, the sequence $\{z_k\}_{k=0}^N$ defined by $z_{k+1} = f(z_k, \mu(z_k, k)) + w_k$, $k \in [0; N-1]$, satisfies $z_k \in \mathcal{X}_\mathrm{o} \setminus \mathcal{X}_\mathrm{u}$, for all $k \in [0; N]$, and $z_N \in \mathcal{X}_\mathrm{t}$.

The definitions of the sets $\mathcal{X}_\mathrm{i}$, $\mathcal{X}_\mathrm{o}$, $\mathcal{X}_\mathrm{u}$, $\mathcal{X}_\mathrm{t}$, $\mathcal{U}$, and $\mathcal{W}$, the nominal sequences $\{\tilde{x}_k\}_{k=0}^N$ and $\{\tilde{u}_k\}_{k=0}^{N-1}$, and all the associated assumptions are fixed throughout the subsequent discussion.

Remark 1: According to (2), we require the nominal states to be in the interior of the operating domain, while being outside the unsafe set, and the final nominal state value to be in the interior of the target set. These conditions will ensure the existence of positive margins surrounding the nominal states that allow backward reachability computations using full-dimensional sets.

IV. Proposed method

In this section, we discuss thoroughly the machinery of our proposed approach, which addresses Problem 1.

A. Constructing state and input tubes

The first element in our proposed approach relies on constructing state and input tubes that surround the given nominal states and inputs. As mentioned before, the tubes will serve two roles: first they will be used to estimate linearization errors, and second, the tubes will serve as safe regions through which backward computations are executed. In particular, we aim to compute sequences of hyper-rectangles $\{\mathcal{T}_{x,k}\}_{k=0}^{N}$ and $\{\mathcal{T}_{u,k}\}_{k=0}^{N-1}$, where $\mathcal{T}_{x,k} \subseteq \mathbb{R}^n,\ k \in [0;N]$, $\mathcal{T}_{u,k} \subseteq \mathbb{R}^m,\ k \in [0;N-1]$, satisfying:

$$\begin{aligned} &\mathrm{center}(\mathcal{T}_{x,k}) = \tilde{x}_k,\ \mathrm{radius}(\mathcal{T}_{x,k}) > 0_n,\ k \in [0;N],\\ &\mathrm{center}(\mathcal{T}_{u,k}) = \tilde{u}_k,\ \mathrm{radius}(\mathcal{T}_{u,k}) \geq 0_m,\ k \in [0;N-1],\\ &\qquad \mathcal{T}_{x,k} \subseteq \mathcal{X}_{\mathrm{o}} \setminus \mathcal{X}_{\mathrm{u}},\ k \in [0;N],\ \mathcal{T}_{x,N} \subseteq \mathcal{X}_{\mathrm{t}},\\ &\qquad \mathcal{T}_{u,k} \subseteq \mathcal{U},\ k \in [0;N-1]. \end{aligned} \tag{3}$$

First, we state and prove some technical results that will be useful in the construction of the state and input tubes.

Lemma 2: Let $v \in [\![a,b]\!] \subseteq \mathbb{R}^p$, where $a, b \in \mathbb{R}^p$, $a \leq b$, then $\mathcal{H}(v, [\![a,b]\!]) \subseteq [\![a,b]\!]$, where

$$\mathcal{H}(v, [\![a,b]\!]) := v + [\![-r, r]\!], \tag{4}$$

and $r = \mathrm{radius}([\![a,b]\!]) - |\mathrm{center}([\![a,b]\!]) - v|$.

Proof: For any $z \in \mathbb{R}^p$, with $|z - v| \leq r$, $|z - \mathrm{center}([\![a,b]\!])| \leq |z - v| + |v - \mathrm{center}([\![a,b]\!])| \leq \mathrm{radius}([\![a,b]\!]) - |\mathrm{center}([\![a,b]\!]) - v| + |\mathrm{center}([\![a,b]\!]) - v| = \mathrm{radius}([\![a,b]\!])$. ■

Lemma 3: Let $x \in \mathbb{R}^p$ and $[\![a,b]\!] \subseteq \mathbb{R}^p$, where $a, b \in \mathbb{R}^p$, $a \leq b$, and $x \notin [\![a,b]\!]$. Moreover, let $r = \mathrm{radius}([\![a,b]\!])$ and $c = \mathrm{center}([\![a,b]\!])$. Then, $\min_{y \in [\![a,b]\!]} \|x - y\|_\infty = \|x - y^*\|_\infty$, where

$$y_i^* := \begin{cases} x_i,\ x_i \in [a_i, b_i], \\ c_i + r_i \mathrm{sgn}(x_i - c_i),\ \text{otherwise}, \end{cases}$$

and $\mathrm{sgn}(\cdot)$ is the signum function. Moreover, let $\tilde{i} \in [1;p]$ such that $|x_{\tilde{i}} - y^*_{\tilde{i}}| = \|x - y^*\|_\infty := M$, and define

$$\mathcal{S}(x, [\![a,b]\!], \alpha) := \{z \in \mathbb{R}^p \,|\, |z_{\tilde{i}} - x_{\tilde{i}}| \leq \alpha M\}, \tag{5}$$

where $\alpha \in [0, 1[$. Then, $\mathcal{S}(x, [\![a,b]\!], \alpha) \cap [\![a,b]\!] = \emptyset$[1].

Proof: The first claim follows by noting that, for all $y \in [\![a,b]\!]$, $|x_i - y_i^*| \leq |x_i - y_i|$, $i \in [1;p]$. For the second claim, note that $M > 0$ as $x \notin [\![a,b]\!]$. Let $z \in \mathcal{S}(x, [\![a,b]\!], \alpha)$, then $|z_{\tilde{i}} - x_{\tilde{i}}| \leq \alpha M < M$. Assume, without loss of generality, that $x_{\tilde{i}} \geq c_{\tilde{i}}$, then it holds, using the definition and minimal property of y^*, that $x_{\tilde{i}} - c_{\tilde{i}} \geq M + r_{\tilde{i}}$. Consequently, $z_{\tilde{i}} - c_{\tilde{i}} = z_{\tilde{i}} - x_{\tilde{i}} + x_{\tilde{i}} - c_{\tilde{i}} \geq -|z_{\tilde{i}} - x_{\tilde{i}}| + M + r_{\tilde{i}} > -M + M + r_{\tilde{i}} = r_{\tilde{i}}$. Hence, $|z_{\tilde{i}} - c_{\tilde{i}}| > r_{\tilde{i}}$, implying $z \notin [\![a,b]\!]$. ■

[1]The set $\mathcal{S}(x, [\![a,b]\!], \alpha)$ is a hyper-rectangle of the form $x + [\![-r, r]\!]$, where $r_{\tilde{i}} = \alpha M$ and $r_i = \infty,\ i \neq \tilde{i}$.

Remark 2: When $[\![a,b]\!]$ is a subset of the unsafe set $\mathcal{X}_{\mathrm{u}}$, $\mathcal{S}(x, [\![a,b]\!], \alpha)$, which satisfies $\mathcal{S}(x, [\![a,b]\!], \alpha) \cap [\![a,b]\!] = \emptyset$, can be thought of as a partially safe region of operation, ensuring not reaching the set $[\![a,b]\!]$, and that will be important for safety guarantees of our backward computations.

From Lemmas 2 and 3, we deduce:

Corollary 1: Let $y \in \mathcal{X}_{\mathrm{o}} \setminus \mathcal{X}_{\mathrm{u}}$, fix $\alpha \in [0, 1[$, and define

$$\mathfrak{R}(y, \mathcal{X}_{\mathrm{o}}, \mathcal{X}_{\mathrm{u}}, \alpha) := \mathcal{H}(y, \mathcal{X}_{\mathrm{o}}) \bigcap \left(\cap_{i=1}^{N_{\mathrm{u}}} \mathcal{S}(y, [\![\underline{x}_{\mathrm{u}}^{(i)}, \overline{x}_{\mathrm{u}}^{(i)}]\!], \alpha) \right). \tag{6}$$

Then, $\mathfrak{R}(y, \mathcal{X}_{\mathrm{o}}, \mathcal{X}_{\mathrm{u}}, \alpha) \subseteq \mathcal{X}_{\mathrm{o}} \setminus \mathcal{X}_{\mathrm{u}}$.

Using the above results, we illustrate in the below theorem, whose proof is omitted for brevity, how state and input tubes are computed.

Theorem 4: Consider the nominal state and input sequences satisfying (2). Fix $\alpha \in [0, 1[$ and define $\mathcal{T}_{x,N} = \mathcal{H}(\tilde{x}_N, \mathcal{X}_{\mathrm{t}})$, $\mathcal{T}_{x,k} = \mathfrak{R}(\tilde{x}_k, \mathcal{X}_{\mathrm{o}}, \mathcal{X}_{\mathrm{u}}, \alpha),\ i \in [0;N-1]$, $\mathcal{T}_{u,k} = \mathcal{H}(\tilde{u}_k, \mathcal{U}),\ i \in [0;N-1]$, then $\{\mathcal{T}_{x,k}\}_{k=0}^{N},\ \{\mathcal{T}_{u,k}\}_{k=0}^{N-1}$ satisfy (3).

B. Linearization

The second element of our approach relies on conservative linearization of the dynamics of system (1) along the nominal state and input sequences. To this end, define the following linearization parameters for all $k \in [0;N-1]$:

$$\begin{aligned} A_k &:= D_x f(\tilde{x}_k, \tilde{u}_k),\ B_k := D_u f(\tilde{x}_k, \tilde{u}_k),\\ c_k &:= f(\tilde{x}_k, \tilde{u}_k) - A_k \tilde{x}_k - B_k \tilde{u}_k, \end{aligned} \tag{7}$$

where $D_u f$ denotes the partial derivative of f with respect to u. Note that based on the assumption on $D_x f$, A_k is invertible for all $k \in [0;N-1]$.

Quantifying linearization error: As we aim to compute backward reachable sets through the tubes discussed above, it is important to quantify linearization errors in subsets of the aforementioned tubes. In the lemma below, which is similar in spirit to results in the framework of hybridization for nonlinear systems [11], [12], we quantify the errors in linearizing the dynamics of system (1) at $\tilde{x}_k$ and $\tilde{u}_k$, $k \in [0;N-1]$, for state and input values neighboring these nominal values.

Lemma 5: Fix $k \in [0;N-1]$ and let $\mathsf{T}_{x,k} = \tilde{x}_k + [\![-\mathsf{r}_x, \mathsf{r}_x]\!] \subseteq \mathbb{R}^n$, where $\mathsf{r}_x \in \mathbb{R}^n_+$, and $\mathsf{T}_{u,k} = \tilde{u}_k + [\![-\mathsf{r}_u, \mathsf{r}_u]\!] \subseteq \mathbb{R}^m$, where $\mathsf{r}_u \in \mathbb{R}^m_+$. For any $(x, u) \in \mathsf{T}_{x,k} \times \mathsf{T}_{u,k}$, $f(x, u) + \mathcal{W} \subseteq A_k x + B_k u + c_k + \mathsf{W}(\mathsf{T}_{x,k}, \mathsf{T}_{x,k})$, where

$$\begin{aligned} \mathsf{W}(\mathsf{T}_{x,k}, \mathsf{T}_{u,k}) &:= \mathcal{W} + [\![-\mathsf{e}(\mathsf{T}_{x,k}, \mathsf{T}_{u,k}), \mathsf{e}(\mathsf{T}_{x,k}, \mathsf{T}_{u,k})]\!],\\ \{\mathsf{e}(\mathsf{T}_{x,k}, \mathsf{T}_{u,k})\}_i &:= \frac{1}{2} [\mathsf{r}_x^\top, \mathsf{r}_u^\top] \bar{\mathrm{H}}_{f_i}(\mathsf{T}_{x,k}, \mathsf{T}_{u,k}) [\mathsf{r}_x^\top, \mathsf{r}_u^\top]^\top, \end{aligned} \tag{8}$$

$i \in [1;n]$. Herein, $\bar{\mathrm{H}}_{f_i}(\mathsf{T}_{x,k}, \mathsf{T}_{u,k}) \in \mathbb{R}^{(n+m)\times(n+m)}$ is any matrix that satisfies $\{\bar{\mathrm{H}}_{f_i}(\mathsf{T}_{x,k}, \mathsf{T}_{u,k})\}_{p,q} \geq \sup_{\mathsf{T}_{x,k} \times \mathsf{T}_{u,k}} |\{\mathrm{Hess}[\mathcal{F}_i](\cdot)\}_{p,q}|$, $p, q \in [1;n+m]$, where

$\mathcal{F}\colon \mathbb{R}^{n+m} \to \mathbb{R}^n$ is defined as $\mathcal{F}([x^\top, u^\top]^\top) = f(x,u)$, $x \in \mathbb{R}^n$, $u \in \mathbb{R}^m$, and $\mathrm{Hess}[\mathcal{F}_i](z)$ denotes the Hessian of $\mathcal{F}_i$ evaluated at z.

A naive approach to obtain $\bar{\mathrm{H}}_{f_i}$, which we adopt in our backward computations in Section V, relies on first computing $\mathrm{Hess}[\mathcal{F}_i]$ through symbolic differentiation, and then evaluating $\mathrm{Hess}[\mathcal{F}_i]$ using interval arithmetic computations over the hyper-rectangular domains of interest.

C. Backward computations

The next, and the most important, element in our proposed approach consists of zonotopic backward reachability computations using the state and input tubes and the linearized dynamics derived above. Below, we elaborate on how such computations are executed.

1) Motivation to use backward computations: Fix $k \in [0; N-1]$ and consider hyper-rectangular subsets $\mathsf{T}_{x,k} \subseteq \mathcal{T}_{x,k}$ and $\mathsf{T}_{u,k} \subseteq \mathcal{T}_{u,k}$, centered at $\tilde{x}_k$ and $\tilde{u}_k$, respectively, where $\mathcal{T}_{x,k}$ and $\mathcal{T}_{u,k}$ are computed according to Theorem 4, and we illustrate in Section IV-C.4 how the subsets $\mathsf{T}_{x,k}$ and $\mathsf{T}_{u,k}$ are obtained. Let $S_{k+1} = \tilde{x}_{k+1} + G_x \mathbb{B}_p \subseteq \mathbb{R}^n$, where $G_x \in \mathbb{R}^{n\times p}$ has full row rank, be a zonotopic set that is required to be reached in one step from a neighborhood of the point $\tilde{x}_k$. In view of Lemmas 1 and 5, any element of the set

$$X_{\mathrm{brs},k} = (A_k^{-1}(\Pi + \Theta)) \cap \mathsf{T}_{x,k}, \tag{9}$$

where $\Pi = (S_{k+1} - \mathsf{W}(\mathsf{T}_{x,k}, \mathsf{T}_{u,k}))$ and $\Theta = -(c_k + B_k \mathsf{T}_{u,k})$, can be driven to S_{k+1} under the dynamics of system (1). Such computation can be applied in a recursive fashion, starting from $k = N-1$ with $S_{k+1} = \mathcal{T}_{x,N}$ until reaching $k = 0$ and the resulting sets can be used to synthesize a tracking controller, with values estimated using linear programming (see equation (15)), that drives the system states to the target set safely.

Backward reachable sets, computed according to (9), can be evaluated exactly using polytopes, as they are closed under intersection and Minkowski addition and difference. However, the complexity of the resulting polytopes and the associated computational cost increase drastically with each iteration of the backward computations. Besides polytopes, there are various classes of set representations that can be utilized in backward reachability computations, including ellipsoids, zonotopes, constrained zonotopes, and polynomial zonotopes (see, e.g., [13] and the references therein), where choosing a proper set class should weigh the computational efficiency and accuracy associated with using that class. Zonotopes (i.e., affine transformations of closed unit balls) have been shown to be effective in reachability computations, possessing reasonable accuracy and computational costs [14], [15], [16], [10], [17], [18]. Motivated by the successes of zonotopic implementations in reachability computations, we aim at computing backward reachable sets using zonotopes. However, exact backward reachability computations can not be attained with zonotopes, which create several computational challenges that we aim to address below. It would be interesting to explore, in future works, the possibilities of implementing different classes of sets in backward computations and comparing their performances. In Section V, we compare through a numerical example the performance of the zonotopic backward computations proposed herein with a variant that utilizes constrained zonotopes [19].

2) Under-approximating Minkowski difference: The first challenge associated with the zonotopic backward reachability computations is the Minkowski difference. In general, zonotopes are not closed under Minkowski difference, which motivated developing several approximating approaches in the literature (see [20], [18], [21]). Herein, we present a simple and efficiently computable zonotopic under-approximation of Minkowski difference under certain assumptions on the generators of the considered zonotopes. More accurate approaches may be adopted, with the price of increased computational cost.

Lemma 6: Let $Z_1 = c_1 + G_1\mathbb{B}_p,\ Z_2 = c_2 + G_2\mathbb{B}_q \subseteq \mathbb{R}^r$, where $c_1, c_2 \in \mathbb{R}^r$, $G_1 \in \mathbb{R}^{r\times p}$, and $G_2 \in \mathbb{R}^{r\times q}$. Assume $\mathrm{rank}(G_1) = r$ and $|G_1^\dagger G_2| 1_q \leq 1_p$[2]. Then, $Z_1 \ominus_{\mathbf{ua}} Z_2 \subseteq Z_1 - Z_2$, where

$$Z_1 \ominus_{\mathbf{ua}} Z_2 := c_1 - c_2 + G_1 \mathrm{diag}(1_p - |G_1^\dagger G_2| 1_q)\mathbb{B}_p. \tag{10}$$

Proof: Let $\tilde{Z} := Z_1 \ominus_{\mathbf{ua}} Z_2$ and $D := \mathrm{diag}(1_p - |G_1^\dagger G_2| 1_q)$. Then, $Z_2 + \tilde{Z} = c_2 + G_2\mathbb{B}_q + c_1 - c_2 + G_1 D\mathbb{B}_p = c_1 + G_1 G_1^\dagger G_2 \mathbb{B}_q + G_1 D \mathbb{B}_p = c_1 + G_1[G_1^\dagger G_2, D]\mathbb{B}_{p+q}$. With the imposed assumption and definition of D, we have $\|[G_1^\dagger G_2, D]\|_\infty = 1$. Hence, $Z_2 + \tilde{Z} \subseteq Z_1$. ■

3) Zonotopic under-approximation of intersection: Another challenge associated with the zonotopic backward reachability computations is the intersection operation. Generally, zonotopes are not closed under intersection. Herein, we propose a computationally efficient and reasonably accurate zonotopic under-approximating approach for intersection of zonotopes and hyper-rectangles that share the same center (this is the case in our backward reachability computations).

Lemma 7: Let $Z_1 = x + G\mathbb{B}_p \subseteq \mathbb{R}^r$, where $x \in \mathbb{R}^r$ and $G \in \mathbb{R}^{r\times p}$ has full row rank, and $Z_2 = x + [\![-\mathfrak{r}, \mathfrak{r}]\!] \subseteq \mathbb{R}^r$, where $\mathfrak{r} \in \mathbb{R}^r_+$. Let $\eta \in \mathbb{R}^p_+$ and $\xi \in \mathbb{R}^r_+$ satisfy:

$$\eta + |G^\dagger| \xi \leq 1_p,\ \ |G|\eta + \xi \leq \mathfrak{r}. \tag{11}$$

Then, $x + G\mathrm{diag}(\eta)\mathbb{B}_p + [\![-\xi, \xi]\!] \subseteq Z_1 \cap Z_2$.

Proof: The first inequality of (11) implies that $\mathrm{diag}(\eta)\mathbb{B}_p + G^\dagger \mathrm{diag}(\xi)\mathbb{B}_r \subseteq \mathbb{B}_p$; hence, $G\mathrm{diag}(\eta)\mathbb{B}_p + [\![-\xi, \xi]\!] \subseteq G\mathbb{B}_p$. Moreover, the second inequality of (11) indicates that $G\mathrm{diag}(\eta)\mathbb{B}_p + [\![-\xi, \xi]\!] \subseteq [\![-\mathfrak{r}, \mathfrak{r}]\!]$. ■

Based on the previous result, we embed the linear constraints (11) in a linear program to obtain a zonotopic under-approximation of the intersection, where the associated objective function was chosen, based on numerical trials, to maximize the size of the under-approximation. Given $Z_1 = x + G\mathbb{B}_p,\ Z_2 = x + [\![-\mathfrak{r}, \mathfrak{r}]\!] \subseteq \mathbb{R}^r$, where $x \in \mathbb{R}^r$

[2]This assumption requires the generators matrix of Z_2 to be sufficiently small norm-wise. For example, the assumption holds if $\|G_2\|_\infty \leq 1/\|G_1^\dagger\|_\infty$. In our backward computations (see equation (9)), Z_2 accounts for disturbances and linearization errors. Hence, this assumption holds for sufficiently small linearization errors and disturbances.

and $G \in \mathbb{R}^{r\times p}$ has full row rank, we define

$$Z_1 \cap_{\mathbf{ua}} Z_2 := x + G\mathrm{diag}(\eta^*)\mathbb{B}_p + [\![-\xi^*, \xi^*]\!], \tag{12}$$

where $(\eta^*, \xi^*) \in \arg\max_{(\eta,\xi)\in\mathbb{R}^p_+\times\mathbb{R}^r_+} \sum_{j=1}^p \eta_j + \sum_{j=1}^r \xi_j$ s.t. (11) and the condition $\eta \geq \alpha_{\min} 1_p$ hold. Herein, $\alpha_{\min} := \min\{\varepsilon \min(\mathfrak{r})/\|G\|_\infty, 1\}$, and $\varepsilon \in \;]0,1]$[3]. Based on the zonotopic under-approximations of the Minkowski difference and intersection, we define the one-step under-approximate backward reachability operator $\mathcal{R}_k$ at time k as

$$\mathcal{R}_k(T_x, T_u, S) := (A_k^{-1}(\Phi + \Psi)) \cap_{\mathbf{ua}} T_x, \tag{13}$$

where $\Phi = S \ominus_{\mathbf{ua}} \mathsf{W}(T_x, T_u)$, $\Psi = -(c_k + B_k T_u)$, T_x and T_u are state and input hyper-rectangles, respectively, and S is a full-dimensional zonotope, where it is guaranteed by construction that T_x and $(A_k^{-1}(\Phi+\Psi))$ share the same center.

Remark 3: In the zonotopic under-approximations of Minkowski difference and intersection presented above, we have utilized Moore-Penrose inverses due to the computational efficiency associated with their evaluations. These inverses may be replaced with other generalized inverses to increase accuracy, with the price of increased computational costs.

4) Scaling the state and input tubes: Let us recall again the definition of the backward reachable set $X_{\mathrm{brs},k}$ in equation (9). Note that the sizes of the hyper-rectangles $\mathsf{T}_{x,k}$ and $\mathsf{T}_{x,k}$ have complex effects on the size of the set $X_{\mathrm{brs},k}$. This is due to the fact that the size of $\mathsf{W}(\mathsf{T}_{x,k}, \mathsf{T}_{x,k})$ correlates with the sizes of the hyper-rectangles $\mathsf{T}_{x,k}, \mathsf{T}_{x,k}$, where the set $\mathsf{W}(\mathsf{T}_{x,k}, \mathsf{T}_{x,k})$ has a deteriorating effect on the size of the resulting backward reachable set. On the other hand, increasing the sizes of the boxes $\mathsf{T}_{x,k}, \mathsf{T}_{x,k}$ will lead to increasing the sizes of the intermediate set resulting from the Minkowski sum expression, and the set to be intersected with. To address this issue, we propose a heuristic procedure, wherein we obtain hyper-rectangular sets $\mathsf{T}_{x,k}$ and $\mathsf{T}_{x,k}$ using a routine denoted $\mathsf{OptimizedBoxes}_k$, i.e., $(\mathsf{T}_{x,k}, \mathsf{T}_{u,k}) = \mathsf{OptimizedBoxes}_k(\mathcal{T}_{x,k}, \mathcal{T}_{u,k}, S_{k+1})$, where $(\mathsf{T}_{x,k}, \mathsf{T}_{x,k})$ results from gradually scaling down $(\mathcal{T}_{x,k}, \mathcal{T}_{u,k})$ and optimizing an estimate of the backward reachable set size. Let $p_x^{(0)} = \mathrm{radius}(\mathcal{T}_{x,k})$, $p_u^{(0)} = \mathrm{radius}(\mathcal{T}_{u,k})$, and let the scaling matrix $\Delta_{\mathrm{sc}} = \mathrm{diag}(\delta_{\mathrm{sc}})$ be given, where $\delta_{\mathrm{sc}} \in [\![0_{n+m}, 1_{n+m}]\!]$ (δ_{sc} can be either determined manually or obtained by solving an auxiliary optimization problem) and $N_{\mathrm{sc,max}}$ be the user-defined maximum number of scaling iterations. Moreover, define $\begin{pmatrix} p_x^{(i)} \\ p_u^{(i)} \end{pmatrix} = \Delta_{\mathrm{sc}} \begin{pmatrix} p_x^{(i-1)} \\ p_u^{(i-1)} \end{pmatrix}$, $\mathsf{T}_x^{(i)} = \tilde{x}_k + [\![-p_x^{(i)}, p_x^{(i)}]\!]$, $\mathsf{T}_u^{(i)} = \tilde{u}_k + [\![-p_u^{(i)}, p_u^{(i)}]\!]$, $i \in [0; N_{\mathrm{sc,max}}]$. Let the function $\tilde{\mathrm{size}}$ be user-defined, where it provides an estimate of the zonotopic size (e.g., $\tilde{\mathrm{size}}(Z)$ is an estimate of the volume of Z). The routine $\mathsf{OptimizedBoxes}_k$ looks for a local maximum of the function $\tilde{\mathrm{size}}$ over the interval $[0; N_{\mathrm{sc,max}}]$, and returns the state and input boxes corresponding to this maximum value, where it runs as follows:

Algorithm 1: $\mathsf{OptimizedBoxes}_k$ routine.

$i \leftarrow 1$, $m \leftarrow \tilde{\mathrm{size}}(\mathcal{R}_k(\mathsf{T}_x^{(0)}, \mathsf{T}_u^{(0)}, S_{k+1}))$,
$\mathsf{T}_{x,k} \leftarrow \mathsf{T}_x^{(0)}$, $\mathsf{T}_{u,k} \leftarrow \mathsf{T}_u^{(0)}$.
while $\underline{i \leq N_{\mathrm{sc,max}}}$ **do**
  $s \leftarrow \tilde{\mathrm{size}}(\mathcal{R}_k(\mathsf{T}_x^{(i)}, \mathsf{T}_u^{(i)}, S_{k+1}))$.
  if $\underline{s \geq m}$ **then**
    $\mathsf{T}_{x,k} \leftarrow \mathsf{T}_x^{(i)}$, $\mathsf{T}_{u,k} \leftarrow \mathsf{T}_u^{(i)}$.
  else
    break.
  end
  $i \leftarrow i + 1$.
end
Result: $(\mathsf{T}_{x,k}, \mathsf{T}_{u,k})$.

5) Zonotopic order reduction: The final challenge in the iterative backward computations is the presence of repeated Minkowski additions, which increases the complexity of resulting zonotopes (Minkowski addition corresponds to concatenation of the generators matrices). This issue can be overcome by using order-reduction techniques, replacing the resulting zonotopes with zonotopic subsets of reduced orders (see, e.g., [20], [18]). In this work, we simply adopt order-reduction techniques from the literature, where we utilize a routine denoted $\mathsf{OrderReduction}$. Given a zonotope $Z = c + G\mathbb{B} \subseteq \mathbb{R}^n$, with order p/n, $\mathsf{OrderReduction}(Z, o)$ yields a zonotope $c + G'\mathbb{B}_{p'} \subseteq Z$, where $p'/n \leq \min\{o, p/n\}$.

Now, we have all the ingredients that allow us to conduct zonotopic backward reachability computations, which are summarized in Theorem 8, whose proof follows from the definitions of the backward reachable sets and is omitted for brevity.

Theorem 8: Fix $\alpha \in [0, 1[$ and let $\mathcal{T}_{x,k},\ k \in [0; N]$ and $\mathcal{T}_{x,k},\ k \in [0; N-1]$ be computed according to Theorem 4. Moreover, fix $o \in \mathbb{R}_+$ and let $\Lambda_i,\ i = N, N-1, \cdots, 0$ be computed as follows: $\Lambda_N = \mathcal{T}_{x,N}$, and

$$\begin{aligned}(\mathsf{T}_{x,k}, \mathsf{T}_{u,k}) &= \mathsf{OptimizedBoxes}_k(\mathcal{T}_{x,k}, \mathcal{T}_{u,k}, \Lambda_{k+1}),\\ \Lambda_k &= \mathsf{OrderReduction}(\mathcal{R}_k(\mathsf{T}_{x,k}, \mathsf{T}_{u,k}, \Lambda_{k+1}), o),\end{aligned} \tag{14}$$

$k \in [0; N-1]$. Assume $\Lambda_0 \neq \emptyset$. Then, $\mathcal{X}_{\mathrm{i}} \cap \Lambda_0 \neq \emptyset$. Moreover, there exists a controller $\mu\colon \mathbb{R}^n \times [0; N-1] \to \mathcal{U}$ such that for any realization of the disturbance given by the sequence $\{w_k\}_{k=0}^{N-1}$, where $w_k \in \mathcal{W},\ k \in [0; N-1]$, and any $z_0 \in \Lambda_0$, the sequence $\{z_k\}_{k=0}^N$ defined by $z_{k+1} = f(z_k, \mu(z_k, k)) + w_k,\ k \in [0; N-1]$, satisfies $z_k \in \mathcal{X}_{\mathrm{o}} \setminus \mathcal{X}_{\mathrm{u}}$ for all $k \in [0; N]$, and $z_N \in \mathcal{X}_{\mathrm{t}}$.

D. Tracking controller computations

The final element in our approach is deducing a tracking controller from the computed backward reachable sets. The tracking control policy μ is obtained by solving the following

[3] The additional condition ensures the full-dimensionality of the resulting under-approximation. Note that, assuming G has full row rank and $\mathfrak{r} > 0_r$, $x + G\mathrm{diag}(\alpha_{\min} 1_p)\mathbb{B}_p$ is a full-dimensional subset of $Z_1 \cap Z_2$. This is due to the facts that $0 < \alpha_{\min} \leq 1$ and $\alpha_{\min} \sum_{j=1}^p |G_{i,j}| \leq \mathfrak{r}_i,\ i \in [1; p]$.

linear program online at each time step:

$$x \in \Lambda_k \Rightarrow \mu(x) \in \operatorname{argmin}_{u \in \mathsf{T}_{u,k}} \|u\|_\infty \text{ s.t.} \\ A_k x + B_k u + c_k \subseteq \Lambda_{k+1} \ominus_{\mathrm{ua}} \mathsf{W}(\mathsf{T}_{x,k}, \mathsf{T}_{u,k}), \tag{15}$$

where the feasibility of the linear program follows from the definition of the sets $\Lambda_k,\ k \in [0; N]$, in Theorem 8.

Some possible modifications can be introduced to (15) in order to enlarge the set of feasible control inputs. For example, the term $\mathsf{W}(\mathsf{T}_{x,k}, \mathsf{T}_{u,k})$, can be replaced with its subset $\mathsf{W}(\mathbf{IH}(\Lambda_k), \mathsf{T}_{u,k})$, where $\mathbf{IH}$ denotes the interval hull operator. Moreover, if system (1) is affine in control (i.e., $f(x,u) = f_0(x) + f_1(x)u$), then the condition $A_k x + B_k u + c_k \subseteq \Lambda_{k+1} \ominus_{\mathrm{ua}} \mathsf{W}(\mathsf{T}_{x,k}, \mathsf{T}_{u,k})$ can be replaced by the less conservative one $f_0(x) + f_1(x)u \subseteq \Lambda_{k+1} \ominus_{\mathbf{ua}} \mathcal{W}$.

V. Numerical Examples

In this section, we illustrate our proposed approach through two numerical examples. The proposed method was implemented in MATLAB (2019a)[4] and run on an AMD Ryzen 5 2500U/2GHz processor. Plots of and order-reduction operations on zonotopes were produced with the help of the software CORA (2022 version) [22]. For order-reduction computations, we used the method `sum` in CORA, which is based on replacing the generators of a zonotope by their sums (see [20], [18]). The bounds of the Hessian, given by $\bar{\mathrm{H}}_{f_i}$, used in estimating the linearization errors, were obtained using interval arithmetic. The linear programs associated with the intersection and tracking control computations were solved using the `linprog` function and the dual simplex method.

A. Dubin's car

Consider the discrete-time Dubin's car system given by:

$$\begin{pmatrix} x_{1,k+1} \\ x_{2,k+1} \\ x_{3,k+1} \end{pmatrix} \in \begin{pmatrix} x_{1,k} + \tau_s u_{1,k} \cos(x_{3,k}) \\ x_{2,k} + \tau_s u_{1,k} \sin(x_{3,k}) \\ x_{3,k} + \tau_s u_{2,k} \end{pmatrix} + \mathcal{W}, \tag{16}$$

where $(x_{1,k}, x_{2,k})$ denotes the car position, $x_{3,k}$ denotes the heading angle, τ_s is the sampling time ($\tau_s = 0.01$), $u_{1,k}$ and $u_{2,k}$ are control inputs corresponding to the car speed and turning rate, respectively, and the disturbance set is given by $\mathcal{W} = \tau_s([-0.02, 0.02]^2 \times [-0.1, 0.1])$. Herein, we illustrate how our approach can be used to synthesize a tracking controller that keeps the states of the car's model in the operating domain $\mathcal{X}_{\mathrm{o}} = [0,5] \times [0,2] \times [-\pi/2, \pi/2]$, while avoiding the unsafe set $(([1.5,3] \times [0,0.5]) \cup ([1.5,2.5] \times [1,2]) \cup ([3.5,4.5] \times [0,1])) \times [-\pi/2, \pi/2]$, and steers the system's states to the target set $\mathcal{X}_{\mathrm{t}} = [3.5,5] \times [1.5,2] \times [-\pi/5, \pi/5]$, starting from the initial set $\mathcal{X}_{\mathrm{i}} = \{(0.5, 1.5, -\pi/4)^\top\}$, using control values in the set $\mathcal{U} = [-8,8] \times [-5,5]$.

The nominal states and inputs were generated using a sampling-based planning approach with steering (see, e.g., [23]), where the nominal trajectory is depicted in Figure 1. We note that in the planning procedure, deflated versions of the safe and target sets and an inflated version of the unsafe set were considered in order to obtain a trajectory satisfying (2). The computational time required to obtain that particular nominal trajectory is approximately 28 seconds, where the value of N obtained from the planning is 260 seconds.

Next, we computed the input and state tubes according to Theorem 4, where we set $\alpha = 0.99$. We obtained the tubes (see Figure 1) in approx. 0.03 seconds, which indicates the minute computational requirements for computing the input and state tubes.

We then proceeded with the backward computations according to Theorem 8. For the intersection under-approximations, we used (12) with $\varepsilon = 0.2$. For the order reduction step, we set $o = 30$ (resulting zonotopes from backward computations are of order 30 at most). For the $\mathsf{OptimizedBoxes}$ routine, we set $N_{\mathrm{sc,max}} = 1000$, and $\delta_{\mathrm{sc}} = (1, 1, 0.7, 0.7, 1)^\top$, where this value was chosen as the remainder error from the linearization (see the definition of W) depends on the heading angle and the input car velocity only. We defined $\tilde{\mathrm{size}}(Z)$, with $Z = c + G\mathbb{B}_p$ being a full-dimensional zonotope, as $1/\|G^\dagger\|_\infty$ (the radius of a particular closed ball contained in Z[5]). The backward reachable sets are depicted in Figure 1, where the associated computational time is approximately 36 seconds, which is reasonable given the time horizon $[0; N]$.

Starting from the set Λ_0 (which contains the singleton initial set), we computed a trajectory of the perturbed dynamics of the Dubin's model, where a tracking controller obtained according to a less conservative version of (15) (see the discussion below equation (15)), was embedded. The average computational time per controller evaluation is approximately 0.015 seconds, which illustrates the low computational requirement for the tracking controller once backward reachable sets are obtained. The resulting trajectory (see Figure 1) satisfies the desired reach-avoid specifications in the presence of disturbance, highlighting the effectiveness of the proposed method.

As we mentioned previously, it is possible to conduct backward reachable set computations using different set representations such as constrained zonotopes [19], [24], which are more general than zonotopes and are closed under intersection. It can be particularly advantageous to use constrained zonotopes when dealing with safety constraints because the intersection between a constrained zonotopic set and the state tube can be computed exactly, and this may result in larger backward reachable sets when compared to the zonotope-based implementation. However, the complexity of constrained zonotopes increases drastically with intersection operations. Moreover, order reduction for constrained zonotopes is not as efficient as the one for zonotopes.

Herein, we developed a preliminary implementation for backward reachability computations using constrained zonotopes, without incorporating order reduction, and compared it with the zonotope-based computations for the Dubin's car

[4]The implementation can be found in the following link: `https://github.com/mserry91/Tracking_Control_Backward_Reachable_Sets`.

[5]$1/\|G^\dagger\|_\infty \mathbb{B}_n = GG^\dagger/\|G^\dagger\|_\infty \mathbb{B}_n \subseteq G\mathbb{B}_p$.

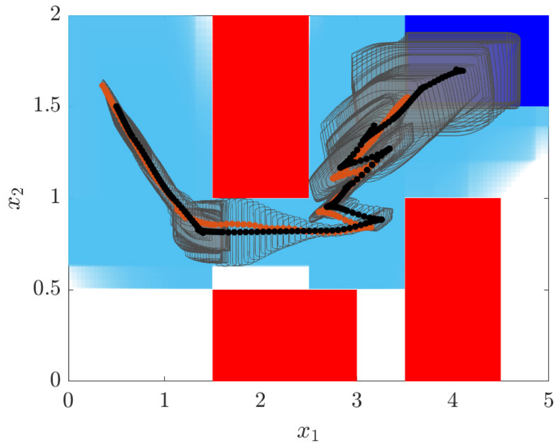

Fig. 1. $x_1 - x_2$ projections of the nominal trajectory for the Dubin's car model (black), state tube (light blue), zonotopic backward reachable sets (gray), and a perturbed trajectory starting from the set Λ_0, where the proposed tracking controller is incorporated (orange). The red boxes correspond to the unsafe set, and the blue box corresponds to the target set.

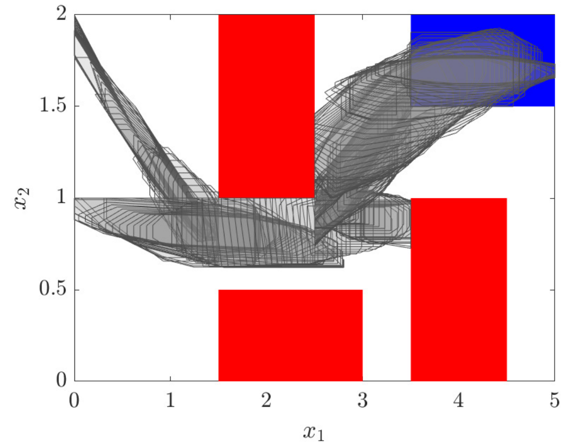

Fig. 2. $x_1 - x_2$ projections of the constrained zonotopic backward reachable sets (gray) associated with Dubin's car example. The red boxes correspond to the unsafe set and the blue box corresponds to the target set.

model. In general, computing the volume of a constrained zonotope is difficult, and the sizes of constrained-zonotopic backward reachable sets depend strongly on the heuristic definition of the function $\widetilde{\text{size}}$ used in the scaling step. For the Dubin's car example, we defined, given a constrained zonotope CZ, $\widetilde{\text{size}}(CZ) = (\overline{x}_1 - \underline{x}_1) \times (\overline{x}_2 - \underline{x}_2) \times (\overline{x}_3 - \underline{x}_3 + 3)$, where $[\![\underline{x}, \overline{x}]\!]$ is a tight hyper-interval containing CZ. Since the x_3-component is responsible for the dynamics' nonlinearity (i.e., the dynamics would be linear if x_3 was constant), we used "+3" in the last term to encourage picking sets with larger x_1-x_2 projections and are thinner in x_3-dimension. This is helpful to avoid large linearization errors that can be induced by large x_3-components. Fig. 2 shows the obtained backward reachable sets represented by constrained zonotopes. In our experiment on an Intel Core i7-10510U/1.8GHz processor, it took 2142 seconds to compute the constrained zonotopic sets, which highlights the large computational demands associated with constrained zonotopes. However, the sizes of the constrained zonotopic sets appear to be larger than the corresponding zonotopic sets, especially after several iterations of the backward computations, which underlines the superior accuracy of constrained zonotopes.

B. Planar quadrotor

Herein, we consider a discrete-time version of the six-dimensional planar quadrotor model studied in [5], [6], [8] obtained using Euler scheme, where

$$\begin{pmatrix} x_{1,k+1} \\ x_{2,k+1} \\ x_{3,k+1} \\ x_{4,k+1} \\ x_{5,k+1} \\ x_{6,k+1} \end{pmatrix} \in \begin{pmatrix} x_{1,k} + \tau_s R_{1,k} \\ x_{2,k} + \tau_s R_{2,k} \\ x_{3,k} + \tau_s R_{3,k} \\ x_{4,k} + \tau_s R_{4,k} \\ x_{5,k} + \tau_s R_{5,k} \\ x_{5,k} + \tau_s R_{6,k} \end{pmatrix} + \mathcal{W}, \qquad (17)$$

$R_{1,k} = x_{4,k}\cos(x_{3,k}) - x_{5,k}\sin(x_{3,k})$, $R_{2,k} = x_{4,k}\sin(x_{3,k}) + x_{5,k}\cos(x_{3,k})$, $R_{3,k} = x_{6,k}$, $R_{4,k} = x_{5,k}x_{6,k} - g\sin(x_{3,k})$, $R_{5,k} = -x_{4,k}x_{6,k} - g\cos(x_{3,k}) + (u_{1,k} + u_{2,k})/m$, $R_{6,k} = l(u_{1,k} - u_{2,k})/J$, $\tau_s = 0.01$, $g = 9.81$, $\mathrm{m} = 0.486$, $l = 0.25$, $J = 0.00383$, $\mathcal{W} = \{0_6\}$[6]. The pair $(x_{1,k}, x_{2,k})$ represents the position, $x_{3,k}$ is the pitch angle, $x_{4,k}$ and $x_{5,k}$ are the quadrotor velocities with respect to the body frame, $x_{6,k}$ is the angular rate, and $u_{1,k}$ and $u_{2,k}$ are the thrust forces from the propellers. Similar to the Dubin's car example, we illustrate the ability of our approach to producing a tracking controller for the quadrotor model satisfying reach-avoid specifications with the accompanying sets: $\mathcal{X}_{\mathrm{o}} = [0,3] \times [0,3] \times [-\pi/3, \pi/3] \times [-3,3] \times [-2,2] \times [-\pi,\pi]$, $\mathcal{X}_{\mathrm{i}} = \{(0.5, 0.5, 0, 0, 0, 0)^\top\}$, $\mathcal{X}_{\mathrm{t}} = [2,3] \times [2,3] \times [-\pi/4, \pi/4] \times [-1,1] \times [-1,1] \times [-\pi/4, \pi/4]$, $\mathcal{X}_{\mathrm{u}} = (([0.25, 1.25] \times [1.5, 2]) \cup ([2, 2.5] \times [0.5, 1.5])) \times ([-\pi/3, \pi/3] \times [-3,3] \times [-2,2] \times [-\pi,\pi])$, $\mathcal{U} = [0, 2\mathrm{mg}]^2$.

We generated a nominal state and input sequences using sampling-based planning (see Figure 3), where the associated computational time is approximately 7 seconds, and the value of N obtained from the planning is 1190.

We then computed the input and state tubes according to theorem 4, with $\alpha = 0.99$, and obtained the tubes (see Figure 3) in approximately 0.05 seconds, which again highlights the minimal computational demands for computing such tubes.

Backward reachable sets were then computed according to Theorem 8. For the intersection under-approximations, we used (12) with $\varepsilon = 0.1$. For the order reduction step, we set $o = 20$ and for the OptimizedBoxes routine, we set $N_{\mathrm{sc,max}} = 3000$, and $\delta_{\mathrm{sc}} = (1, 1, 0.9, 0.85, 0.85, 0.9, 1, 1)^\top$.

[6] For this example, our zonotopic computations were not able to handle nonzero disturbances due to the nonlinearity of the quadrotor model, the large number of steps needed to reach the target set, and the accumulating inaccuracies of zonotopic under-approximations. Still, the zonotopic backward computations with zero disturbance were beneficial as they resulted in a larger 'winning' region, containing the initial point of interest, where all the points in the wining region could be driven to the target set safely.

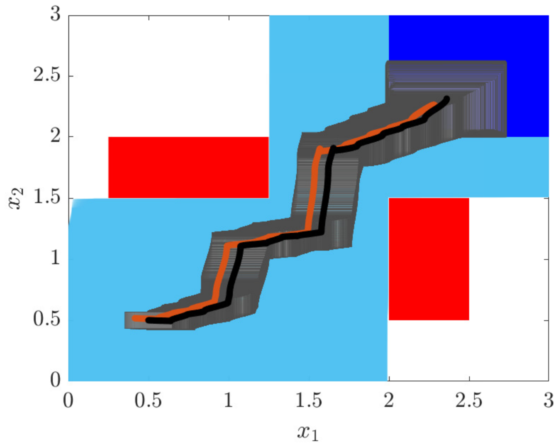

Fig. 3. $x_1 - x_2$ projections of the nominal trajectory for the planar quadrotor model (black), state tube (light blue), zonotopic backward reachable sets (gray), and a trajectory starting from the set Λ_0, where the proposed tracking controller is incorporated (orange). The red boxes correspond to the unsafe set and the blue box corresponds to the target set.

Moreover, $\tilde{\text{size}}(Z)$, with Z being a zonotope had the same definition as in the Dubin's car example. The backward reachable sets are depicted in Figure 3, where the associated computational time is approximately 144 seconds, and that is attributed to the relatively large number of time steps.

A tracking controller (the relaxed version of (15) for affine-in-control systems) was then implemented, and a trajectory starting from the set Λ_0 was computed (see Figure 3). The average computational time per controller evaluation is less than 0.02 seconds, indicating again the efficiency of the online computations associated with the tracking controller. The controller in this example was capable of driving the quadrotor's states to the target set, avoiding the unsafe values and fulfilling the input constraints, which highlights the promising applications of the proposed method.

VI. Conclusion

In this paper, we proposed a new tracking control approach for discrete-time nonlinear uncertain systems under reach-avoid specifications and input/state constraints using zonotope-based backward reachability computations. Through two numerical examples, we illustrated the effectiveness of our approach, where the resulting tracking controllers were safe and robust, and the associated computational requirements were reasonable.

It is of our interest in future work to introduce further refinements to the different aspects of our set-based approach. For example, we seek to develop accurate and computationally efficient zonotopic under-approximations of intersections. Moreover, we aim to derive better heuristics for enlarging the sizes of the backward reachable sets. Furthermore, it would be interesting to extensively explore the effectiveness of different classes of sets, besides zonotopes and constrained zonotopes, in similar set-based backward computations. Finally, we aim to compare our proposed approach with the tracking approaches in the literature to better elucidate its advantages and limitations in control applications.

References

[1] K. Graichen, M. Treuer, and M. Zeitz, "Swing-up of the double pendulum on a cart by feedforward and feedback control with experimental validation," Automatica, vol. 43, no. 1, pp. 63–71, 2007.

[2] T. Lee, M. Leok, and N. H. McClamroch, "Geometric tracking control of a quadrotor uav on se (3)," in Proc. of CDC. IEEE, 2010, pp. 5420–5425.

[3] S. Fukuda, Y. Satoh, and O. Sakata, "Trajectory-tracking control considering obstacle avoidance by using control barrier function," in Proc. of CACS. IEEE, 2020, pp. 1–6.

[4] W. Langson, I. Chryssochoos, S. Raković, and D. Q. Mayne, "Robust model predictive control using tubes," Automatica, vol. 40, no. 1, pp. 125–133, 2004.

[5] S. Singh, B. Landry, A. Majumdar, J.-J. Slotine, and M. Pavone, "Robust feedback motion planning via contraction theory," The International Journal of Robotics Research, 2019.

[6] P. Zhao, A. Lakshmanan, K. Ackerman, A. Gahlawat, M. Pavone, and N. Hovakimyan, "Tube-certified trajectory tracking for nonlinear systems with robust control contraction metrics," IEEE Robotics and Automation Letters, vol. 7, no. 2, pp. 5528–5535, 2022.

[7] S. V. Raković, L. Dai, and Y. Xia, "Homothetic tube model predictive control for nonlinear systems," IEEE Trans. Automatic Control, 2022.

[8] A. Sasfi, M. N. Zeilinger, and J. Köhler, "Robust adaptive mpc using control contraction metrics," Automatica, vol. 155, p. 111169, 2023.

[9] C. Fan, Z. Qin, U. Mathur, Q. Ning, S. Mitra, and M. Viswanathan, "Controller synthesis for linear system with reach-avoid specifications," IEEE Trans. Automatic Control, vol. 67, no. 4, pp. 1713–1727, 2021.

[10] A. Girard, "Reachability of uncertain linear systems using zonotopes," in Proc. of HSCC, vol. 3414. Springer, 2005, pp. 291–305.

[11] E. Asarin, T. Dang, and A. Girard, "Reachability analysis of nonlinear systems using conservative approximation," in Proc. of HSCC. Springer, 2003, pp. 20–35.

[12] M. Althoff, O. Stursberg, and M. Buss, "Reachability analysis of nonlinear systems with uncertain parameters using conservative linearization," in Proc. of CDC. IEEE, 2008, pp. 4042–4048.

[13] M. Althoff, G. Frehse, and A. Girard, "Set propagation techniques for reachability analysis," Annual Review of Control, Robotics, and Autonomous Systems, vol. 4, pp. 369–395, 2021.

[14] A. Girard, C. L. Guernic, and O. Maler, "Efficient computation of reachable sets of linear time-invariant systems with inputs," in Proc. of HSCC. Springer, 2006, pp. 257–271.

[15] M. Serry and G. Reissig, "Over-approximating reachable tubes of linear time-varying systems," IEEE Trans. Automatic Control, vol. 67, no. 1, pp. 443–450, 2021.

[16] M. Serry and J. Liu, "Underapproximate reachability analysis for a class of linear systems with inputs," IEEE Trans. Automatic Control, vol. 69, no. 2, pp. 1125–1132, 2024.

[17] M. Althoff, "Reachability analysis and its application to the safety assessment of autonomous cars," Ph.D. dissertation, Technische Universität München, 7 Jul. 2010.

[18] L. Yang and N. Ozay, "Scalable zonotopic under-approximation of backward reachable sets for uncertain linear systems," IEEE Control Systems Letters, vol. 6, pp. 1555–1560, 2021.

[19] J. K. Scott, D. M. Raimondo, G. R. Marseglia, and R. D. Braatz, "Constrained zonotopes: A new tool for set-based estimation and fault detection," Automatica, vol. 69, pp. 126–136, 2016.

[20] V. Raghuraman and J. P. Koeln, "Set operations and order reductions for constrained zonotopes," Automatica, vol. 139, p. 110204, 2022.

[21] M. Althoff, "On computing the minkowski difference of zonotopes," arXiv preprint arXiv:1512.02794, 2015.

[22] ——, "An introduction to CORA 2015," in Proc. of ARCH, 2015.

[23] S. M. LaValle and J. J. Kuffner Jr, "Randomized kinodynamic planning," The international journal of robotics research, vol. 20, no. 5, pp. 378–400, 2001.

[24] L. Yang, H. Zhang, J.-B. Jeannin, and N. Ozay, "Efficient backward reachability using the minkowski difference of constrained zonotopes," IEEE Trans. Computer-Aided Design of Integrated Circuits and Systems, vol. 41, no. 11, pp. 3969–3980, 2022.